



## Lorenz Hiperkaotik Sisteminin Aktif Kontrol Tabanlı Senkronizasyonu ve Sinyal Maskeleye Uygulaması

Fırat TUNÇ<sup>1</sup> , Erman ÖZPOLAT<sup>2\*</sup> , Vedat ÇELİK<sup>3</sup> 

<sup>1</sup>Elektrik-Elektronik Mühendisliği Anabilim Dalı, Fen Bilimleri Enstitüsü, Fırat Üniversitesi, Elazığ, Türkiye.

<sup>2</sup>Elektrik-Elektronik Mühendisliği, Mühendislik ve Mimarlık Fakültesi, Muş Alparslan Üniversitesi, Muş, Türkiye.

<sup>3</sup>Elektrik-Elektronik Mühendisliği, Mühendislik Fakültesi, Fırat Üniversitesi, Elazığ, Türkiye.

<sup>1</sup>firtnc94@gmail.com, <sup>2</sup>e.ozpolat@alparslan.edu.tr, <sup>3</sup>celik@firat.edu.tr

Geliş Tarihi: 23.03.2026

Kabul Tarihi: 18.05.2026

Düzeltilme Tarihi: 13.04.2026

doi: <https://doi.org/10.62520/fujece.1914159>

Araştırma Makalesi

Alıntı: F. Tunç, E. Özpolat ve V. Çelik, "Lorenz hiperkaotik sisteminin aktif kontrol tabanlı senkronizasyonu ve sinyal maskeleye uygulaması", Fırat Üni. Deny. Müh. Derg., vol. 5, no 2, pp. 519-537, Haziran 2026.

### Öz

Bu çalışma, Lorenz hiperkaotik sisteminin nasıl çalıştığını ve iki özdeş sistemin birlikte çalışmasını sağlamak için aktif kontrolün nasıl kullanılabileceğini incelemektedir. Sistemin hiperkaotik doğasını doğrulamak amacıyla, Lyapunov üsleri, faz uzayı diyagramı ve başlangıç koşullarına duyarlılık üzerinde durularak sistemin dinamik yapısı incelenmiştir. Ardından, sürücü-yanıt gibi çalışan bir senkronizasyon şeması tanıtılmaktadır. Senkronizasyon sürecinin kararlılığını değerlendirmek için ilgili hata dinamikleri kullanılmakta ve kontrol parametrelerinin yakınsama koşulları ve sistem özdeğerleri üzerindeki etkisi analiz edilmektedir. Önerilen yöntemin sadece teorik bir çalışmanın ötesine geçtiğini göstermek için bir sinyal maskeleye ve kurtarma uygulaması incelenmektedir. Kontrolörün açılmasından önce ve sonra sistemin davranışı kontrol edilmektedir. Senkronizasyondan sonra, maskelenmiş form gönderilen sinyali doğru bir şekilde yeniden oluşturmak için kullanılabilir. Farklı giriş sinyallerinin kullanılması da yöntemin ne kadar tutarlı olduğunu test etmektedir. Her durum benzer şekilde işlediğinden, yöntem birçok farklı durumda hala iyi çalışmaktadır. Bu sonuçlar topluca, aktif kontrole dayalı senkronizasyon çerçevesinin Lorenz hiperkaotik sistemi için uygulanabilir ve güvenilir bir çözüm sunduğunu göstermektedir.

**Anahtar kelimeler:** Kaos, Hiperkaotik sistemler, Aktif senkronizasyon, Sinyal maskeleye

\*Yazışılan Yazar

İntihal Kontrol: Evet – Turnitin

Şikayet: [fujece@firat.edu.tr](mailto:fujece@firat.edu.tr)

Telif Hakkı ve Lisans: Dergide yayın yapan yazarlar, CC BY-NC 4.0 kapsamında lisanslanan çalışmalarının telif hakkını saklı tutar.



## Active Control-Based Synchronization of a Lorenz Hyperchaotic System with an Application to Secure Signal Masking

Firat TUNÇ<sup>1</sup> , Eрман ÖZPOLAT<sup>2\*</sup> , Vedat ÇELİK<sup>3</sup> 

<sup>1</sup>Department of Electrical and Electronics Engineering, Graduate School of Natural and Applied Sciences, Firat University, Elazig, Türkiye.

<sup>2</sup>Electrical and Electronics Engineering, Faculty of Engineering and Architecture, Mus Alparslan University, Mus, Türkiye.

<sup>3</sup>Electrical and Electronics Engineering, Faculty of Engineering, Firat University, Elazig, Türkiye.

<sup>1</sup>firtnc94@gmail.com, <sup>2</sup>e.ozpolat@alparslan.edu.tr, <sup>3</sup>celik@firat.edu.tr

Received: 23.03.2026

Accepted: 18.05.2026

Revision: 13.04.2026

doi: <https://doi.org/10.62520/fujece.1914159>

Research Article

Citation: F. Tunç, E. Özpolat and V. Çelik, "Active control-based synchronization of a Lorenz hyperchaotic system with an application to secure signal masking", *Firat Univ. Jour. of Exper. and Comp. Eng.*, vol. 5, no 2, pp. 519-537, June 2026.

### Abstract

This study investigates the dynamics of the Lorenz hyperchaotic system and presents an active control-based synchronization approach for two identical systems. To confirm the hyperchaotic nature of the system, an examination of its dynamic structure is conducted, emphasizing Lyapunov exponents, phase-space evolution, and sensitivity to initial conditions. Subsequently, a synchronization scheme operating as a driver-response is introduced. The associated error dynamics are employed to evaluate the stability of the synchronization process, and the influence of control parameters on convergence conditions and system eigenvalues is analyzed. It is examined that a signal masking and recovery application to show that the proposed method goes beyond just theoretical study. Before and after the controller is turned on, the system's behavior is checked. After synchronization, the masked signal can be used to accurately reconstruct the transmitted signal. The use of different input signals also evaluates the consistency of the proposed method. The proposed method maintains effective performance under various conditions, as each case exhibits similar dynamical behavior. These results collectively demonstrate that the synchronization framework based on active control offers a feasible and dependable solution for the Lorenz hyperchaotic system.

**Keywords:** Chaos, Hyperchaotic systems, Active synchronization, Signal masking

\*Corresponding author

## **1. Introduction**

Chaotic behavior is defined as erratic actions occurring in deterministic systems regulated by differential equations. A primary characteristic of these systems is their high sensitivity to initial conditions. This means that even small changes can lead to very different paths over time [1]. Chaos theory did not receive significant scholarly attention until the second half of the 20th century. Edward Lorenz made one of the first and most important discoveries in the 1960s. He observed that minor alterations in the initial values of atmospheric convection models could result in significantly divergent weather forecasts [2, 3]. This observation subsequently became recognized as the basis of contemporary chaos theory.

Deterministic rules govern chaotic systems, yet their behavior frequently appears highly random and difficult to anticipate. This seeming contradiction has made chaos a major area of study in many fields, such as meteorology, electrical engineering, biology, and secure communication [4, 5]. After the Lorenz attractor was made public in 1963, more studies were done. As a result, several well-known chaotic models were suggested, such as the Rössler system (1976) [6], the Chen system (1999) [7], and the Lü system (2002) [8].

Chaotic systems have been widely employed in various fields for many years. They have been used in biomedical engineering, communication technologies, encryption methods, and optoelectronic and electromagnetic systems [9-14]. This wide range of applications demonstrates the versatility of chaos theory. It is very useful for security-related uses that need to be hard to guess and understand.

Hyperchaotic systems are a kind of classical chaotic system that has more dimensions and more complicated dynamics [15]. Most of the studies before this one were about three-dimensional systems. The discovery of systems with more than one positive Lyapunov exponent led to the development of hyperchaos [16]. The divergence in phase space is stronger when there is more than one positive exponent in these kinds of systems.

Synchronization of chaotic systems is the process by which two or more systems change over time in a coordinated way. Even though initial conditions are very important, it is still possible to achieve synchronization by using the right coupling structures or driver-response (master-slave) setups. The 1990 study by Pecora and Carroll demonstrated that synchronization is feasible, thereby inaugurating a novel trajectory in chaos research [17]. Since that time, many different control-based synchronization methods have been suggested. These are sliding mode control [18], nonlinear active control [19], linear error state feedback control [20], adaptive feedback control [21], cluster synchronization [22], and linear active control techniques [23]. These methods have generally worked well on both systems that are the same and systems that are not.

Linear active control is often the best choice among these methods because it is easy to understand and use. The method uses error dynamics to define the control inputs instead of complicated formulas. This also makes stability analysis easier [24-26]. This is why it is now a common way to sync hyperchaotic systems.

There has been a noticeable rise in interest in active control-based synchronization in the last few years. Various hyperchaotic models have been suggested and examined regarding their dynamic and stability characteristics. For instance, Zhou et al. (2025) [27] developed a five-dimensional hyperchaotic system by augmenting a four-dimensional model with a linear memristor structure and validated its behavior through comprehensive analysis. They also used the system to keep pictures safe. Kopp et al. (2024) [28] created a six-dimensional system based on modified Lorenz equations and used circuit simulations to test their theoretical framework. Özpolat et al. (2024) [29] introduced a novel four-dimensional hyperchaotic system and illustrated its efficacy in secure communication via synchronization and encryption techniques. Lekshmi et al. (2025) [30] introduced a fractional-order hyperchaotic system utilizing the Caputo derivative, demonstrating that active control facilitates rapid and stable synchronization. Although these studies have made significant contributions to the existing body of

knowledge, synchronization performance should still be examined together with the dynamical properties of the system and its applicability to different hyperchaotic models.

Based on this motivation, the main contributions of the present study can be summarized as follows:

- The Lorenz hyperchaotic system is examined in terms of its dynamical behavior, and its hyperchaotic nature is verified through detailed analyses.
- A synchronization structure based on the active control approach is constructed for two identical Lorenz hyperchaotic systems, and the stability of the system is analyzed.
- The effect of control parameters on the eigenvalue distribution is investigated, and the conditions required for asymptotic synchronization are identified.
- A signal masking and recovery application is developed by using the proposed synchronization framework.

The remainder of this paper is organized as follows. Section 2 presents the mathematical model of the Lorenz hyperchaotic system and examines its dynamical behavior over time. Section 3 presents the synchronization process based on the active control method and provides the corresponding stability analysis. Section 4 describes the signal masking and recovery application. Finally, Section 5 summarizes the main findings of the study.

## 2. The Lorenz Hyperchaotic System

In 1961, Edward Lorenz observed unpredictable behavior in deterministic systems while conducting weather prediction studies, which led to a growing interest in the concept of chaos. Initially working on a twelve-variable model, Lorenz later simplified the system into a three-dimensional set of differential equations, which became widely known in the literature as the Lorenz chaotic system. This system was suggested to mathematically model atmospheric phenomena and clearly showed that even tiny changes in the starting conditions could cause big and unpredictable changes over time [3].

After the Lorenz attractor was found in 1963, many more people in academia became interested in chaos theory. Subsequently, numerous new chaotic and hyperchaotic systems were reported in the literature. Equation 1 [3] shows the state equations of the Lorenz chaotic system [3].

$$\begin{aligned}\dot{x} &= \alpha(y - x) \\ \dot{y} &= cx - y - xz \\ \dot{z} &= -bz + xy\end{aligned}\tag{1}$$

In this case,  $\alpha$ ,  $b$  and  $c$  stand for the system parameters, and  $x$ ,  $y$  and  $z$  stand for the system's state variables. The parameter values  $\alpha=10$ ,  $b=8/3$  and  $c=28$  show chaotic behavior. The Lorenz chaotic system, which has a three-dimensional structure and only one positive Lyapunov exponent, shows the basic features of chaotic dynamics. Nonetheless, augmenting the system dimension and acquiring multiple positive Lyapunov exponents facilitates the examination of more intricate and nuanced dynamical behaviors.

The Lorenz hyperchaotic system, an extension of the classical Lorenz system, has emerged as a pivotal focus in chaos theory and engineering applications. To create a hyperchaotic system, incorporate a nonlinear controller term  $\dot{w} = -yz + rw$  into the Lorenz chaotic system [31].

The state equations of the Lorenz hyperchaotic system are presented in Equation 2.

$$\begin{aligned}\dot{x} &= \alpha(y - x) + w \\ \dot{y} &= cx - y - xz \\ \dot{z} &= -bz + xy \\ \dot{w} &= -yz + rw\end{aligned}\tag{2}$$

When the parameter values are selected as  $\alpha = 10, b = 8/3, c = 28$  and  $r = -1$ , the system exhibits hyperchaotic behavior.

### Dynamic analysis of the hyperchaotic system

Dynamic analysis looks at how the states of nonlinear systems change over time and what their natural behavioral properties are. These kinds of studies are useful for determining whether a system is in a stable equilibrium, a periodic regime, a chaotic state, or a hyperchaotic domain. This section analyzes the temporal dynamics of the Lorenz hyperchaotic system by calculating Lyapunov exponents, showing phase-space trajectories, and doing sensitivity analysis with different starting conditions. The outcomes of these analyses are employed to corroborate the hyperchaotic structure of the system.

One of the most important approaches for characterizing hyperchaotic dynamics is the analysis of Lyapunov exponents. A dynamical system is hyperchaotic if it has at least two positive Lyapunov exponents [32]. This means that it diverges in more than one independent direction within phase space. The current study utilizes the numerical method formulated by Alan Wolf, indicating divergence in multiple independent directions within phase space. In the present study, the Lyapunov spectrum is determined using the numerical procedure introduced by Alan Wolf [33] to ascertain the Lyapunov spectrum. The Wolf algorithm checks how different nearby paths are by adding a small change to the system and watching how it changes over time. To keep the numbers stable, the deviation vectors are renormalized from time to time. This stops them from growing or shrinking too much while the computation is going on. This repeated normalization makes it possible to accurately estimate the exponential divergence rates and makes sure that the Lyapunov exponents are calculated in a stable and reliable way.

Figure 1 shows how the Lyapunov exponents for the Lorenz hyperchaotic system change over time. When calculating the Lyapunov exponents, the system's starting conditions are set to [1,1,1,1] with 0.5 step time.

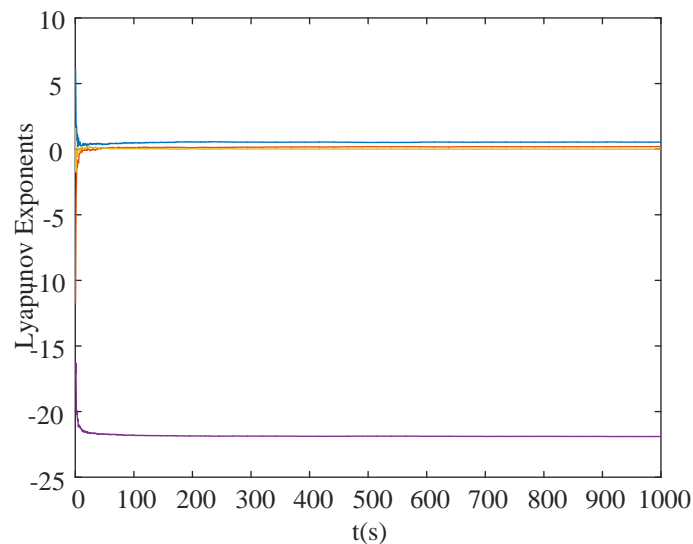


**Figure 1.** Time evolution of the Lyapunov exponents

The Lyapunov exponents calculated for the Lorenz hyperchaotic system are obtained as  $\lambda_1 = 0.539260$ ,  $\lambda_2 = 0.194269$ ,  $\lambda_3 = 0$ ,  $\lambda_4 = -21.894$ . The presence of two positive Lyapunov exponents confirms that the system exhibits hyperchaotic behavior.

The behavior of chaotic systems can be directly observed through phase-space portraits. In this study, the system parameters are selected as  $\alpha = 10, b = 8/3, c = 28$ , and  $r = -1$ , while the initial conditions

are chosen as  $[1,1,1,1]$ . The phase-space portraits obtained for these parameter values are presented in Figure 2, clearly demonstrating the chaotic characteristics of the system.

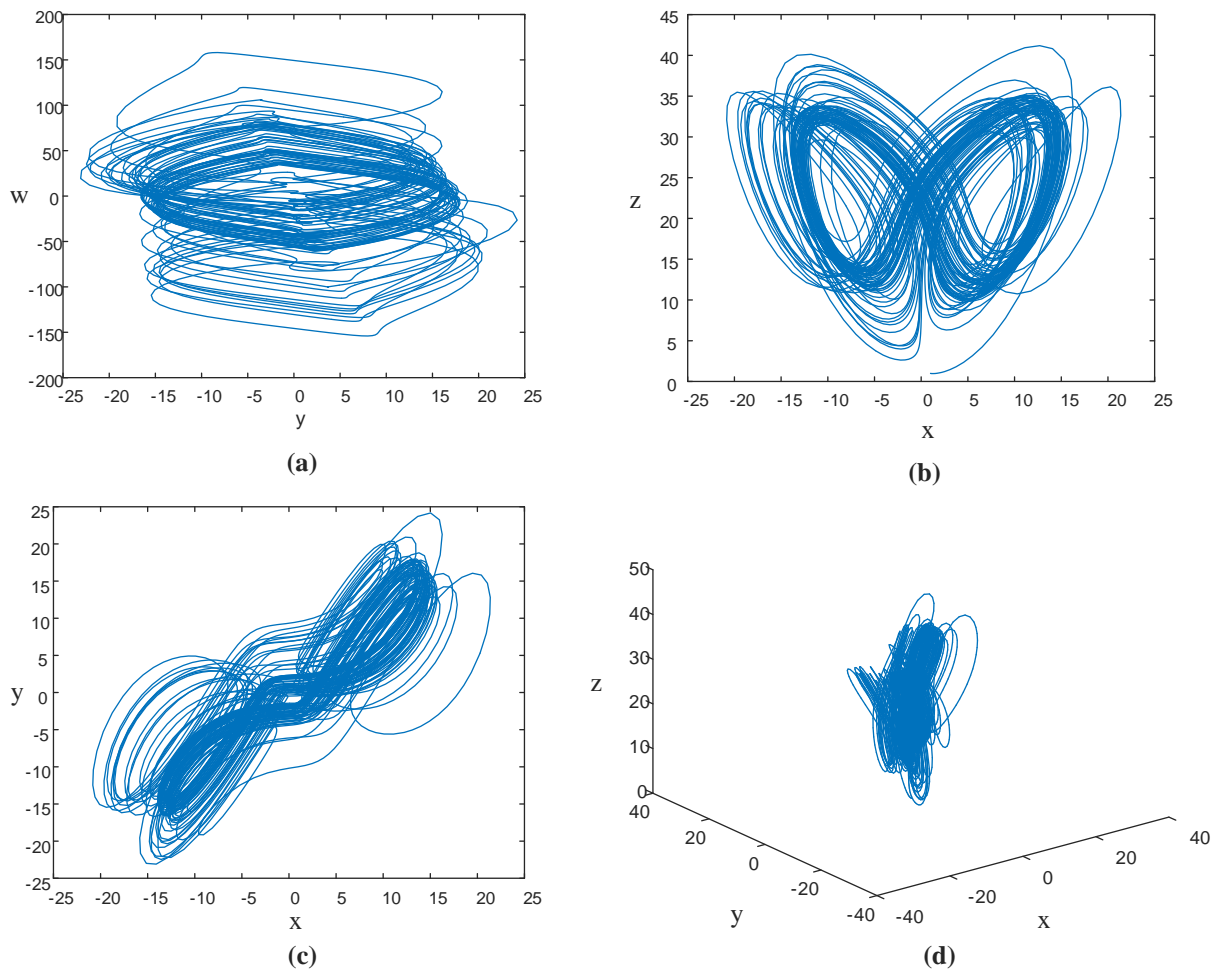


**Figure 2.** Phase-space portraits of the Lorenz hyperchaotic system: (a)  $y$ - $w$  plane, (b)  $x$ - $z$  plane, (c)  $x$ - $y$  plane, and (d) three-dimensional phase-space representation ( $x$ - $y$ - $z$ )

As shown in Figure 2, the chaotic trajectory is observed to vary between -25 and 25 along the  $x$  and  $y$ -axes, between 0 and 45 along the  $z$ -axis, and between -200 and 200 along the  $w$ -axis.

A primary attribute of hyperchaotic systems is their significant sensitivity to initial conditions. Small changes in the starting states can cause the outputs of a system to diverge in ways that cannot be predicted over time. Figure 3 shows how small changes in the initial conditions can cause big changes in how the system behaves.

In this study, the initial conditions of the system are chosen to be  $[1,1,1,1]$  for the first case, and the time series that goes with it is shown in blue. In the second case, the starting conditions are  $[1.01,1,1,1]$ , and the time series that goes with them is shown in red. Both signals act in a similar way for the first 20 seconds or so. After that, though, the two paths start to diverge in a clear way.

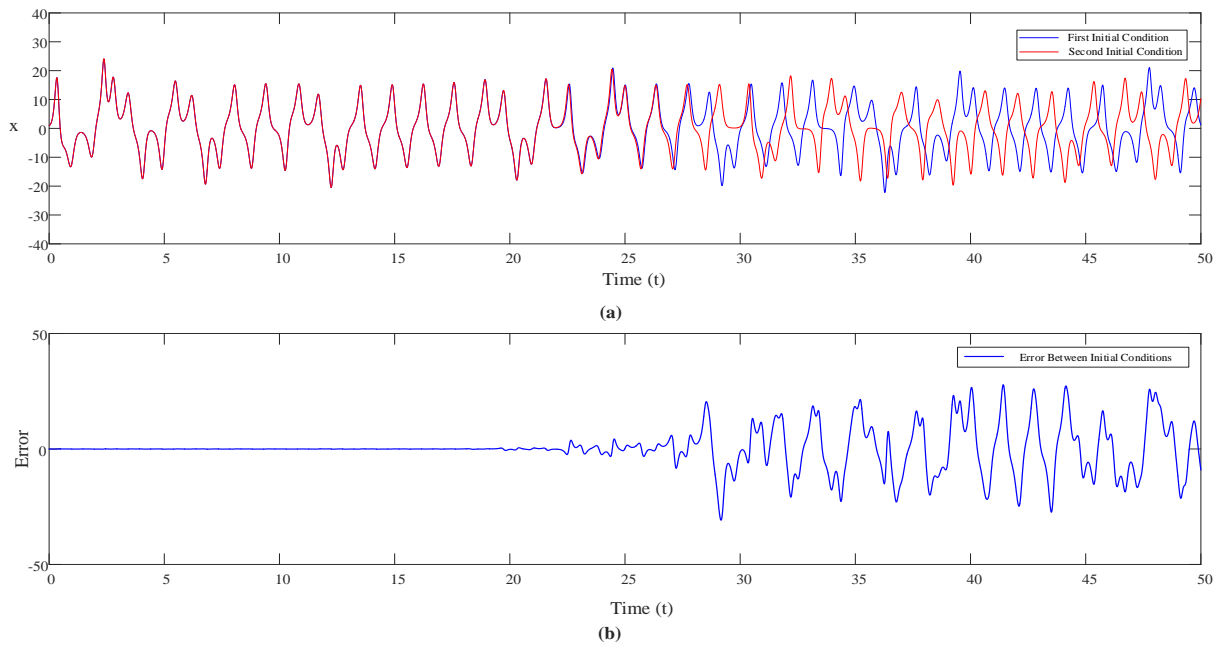


**Figure 3.** How sensitive the Lorenz hyperchaotic system is to its starting conditions: (a) time series for different starting conditions, and (b) how the difference between the two trajectories changes over time

The Lyapunov exponent analysis, phase-space portraits, and sensitivity investigations regarding initial conditions conducted in this section affirm that the Lorenz hyperchaotic system demonstrates hyperchaotic behavior. The results indicate that the system exhibits a nonlinear and intricate dynamical structure.

### 3. Active Synchronization of Two Identical Lorenz Hyperchaotic Systems

This section focuses on the active synchronization of two identical Lorenz hyperchaotic systems by looking at the system's dynamic properties. To achieve this, the driver and response systems are delineated, with the objective of attaining synchronization between them.

Synchronization of dynamical systems refers to the process by which systems with different starting conditions move toward a single, stable behavior over time [34]. Because chaotic systems are by nature unpredictable, uncontrolled dynamics can lead to unintended or unexpected outcomes. Therefore, rather than constructing perfectly identical chaotic systems, extensive research has focused on achieving synchronization between such systems [35-37]. Once synchronized, chaotic systems operate simultaneously and coherently, allowing their dynamics to become observable and controllable.

In the active control approach, appropriate control signals are applied to the response system to ensure that the state variables of the two systems converge over time, thereby driving the synchronization error to zero [38]. The block diagram of the implemented active synchronization scheme is presented in Figure 4.

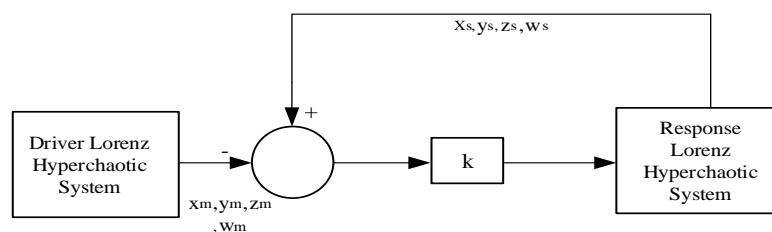


**Figure 4.** Block diagram of the active controller

Using the mathematical model of the Lorenz hyperchaotic system, the governing equations of the driver system are given in Equation 3. The system parameters are chosen as  $\alpha = 10$ ,  $b = 8/3$ ,  $c = 28$ , and  $r = -1$ .

$$\begin{aligned} \dot{x}_m &= 10y_m - 10x_m + w_m \\ \dot{y}_m &= 28x_m - y_m - x_m z_m \\ \dot{z}_m &= -\frac{8}{3}z_m + x_m y_m \\ \dot{w}_m &= -y_m z_m - w_m \end{aligned} \tag{3}$$

Corresponding to the driver Lorenz hyperchaotic system, the equations of the response Lorenz hyperchaotic system are given in Equation 4. In order to achieve synchronization with the driver system, the active control functions  $U_a(t)$ ,  $U_b(t)$ ,  $U_c(t)$ , and  $U_d(t)$  are incorporated into the response system.

$$\begin{aligned} \dot{x}_s &= 10y_s - 10x_s + w_s + U_a(t) \\ \dot{y}_s &= 28x_s - y_s - x_s z_s + U_b(t) \\ \dot{z}_s &= -\frac{8}{3}z_s + x_s y_s + U_c(t) \\ \dot{w}_s &= -y_s z_s - w_s + U_d(t) \end{aligned} \tag{4}$$

The synchronization errors are defined as the differences between the corresponding state variables of the driver and response systems and are denoted as  $e_1$ ,  $e_2$ ,  $e_3$ , and  $e_4$ . The mathematical formulations of these error variables are given in Equation 5.

$$\begin{aligned} e_1 &= x_s - x_m \\ e_2 &= y_s - y_m \\ e_3 &= z_s - z_m \\ e_4 &= w_s - w_m \end{aligned} \tag{5}$$

The time derivatives of the defined error variables are obtained by considering the differences between the driver and response systems. By incorporating the active control functions, the differential equations governing the resulting error dynamics are presented in Equation 6.

$$\begin{aligned} \dot{e}_1 &= 10e_2 - 10e_1 + e_4 + U_a(t) \\ \dot{e}_2 &= 28e_1 - e_2 - x_s z_s + x_m z_m + U_b(t) \\ \dot{e}_3 &= -\frac{8}{3}e_3 + x_s y_s - x_m y_m + U_c(t) \\ \dot{e}_4 &= -y_s z_s + y_m z_m - e_4 + U_d(t) \end{aligned} \tag{6}$$

To stabilize the error dynamics and achieve synchronization, the active control functions applied to the response system are appropriately designed. The control inputs  $U_a(t)$ ,  $U_b(t)$ ,  $U_c(t)$ , and  $U_d(t)$  employed in this study are presented in Equation 7.

$$\begin{aligned} U_a(t) &= v_a(t) \\ U_b(t) &= x_s z_s - x_m z_m + v_b(t) \\ U_c(t) &= -x_s y_s + x_m y_m + v_c(t) \\ U_d(t) &= y_s z_s - y_m z_m + v_d(t) \end{aligned} \tag{7}$$

In order to drive the synchronization error to zero, the auxiliary control signals are designed in the form of negative feedback based on the error variables. Accordingly, the expressions for  $v_a(t)$ ,  $v_b(t)$ ,  $v_c(t)$ , and  $v_d(t)$  are provided in Equation 8.

$$\begin{aligned} v_a(t) &= -k_1 e_1 \\ v_b(t) &= -k_2 e_2 \end{aligned} \tag{8}$$

$$\begin{aligned} v_c(t) &= -k_3 e_3 \\ v_d(t) &= -k_4 e_4 \end{aligned}$$

Here,  $k_1$ ,  $k_2$ ,  $k_3$ , and  $k_4$  denote the positive control gains. By substituting the defined active control functions and feedback laws into the error dynamics, the closed-loop error system is obtained. Accordingly, the differential equations governing the error dynamics under the effect of control are presented in Equation 9.

$$\begin{aligned} \dot{e}_1 &= 10e_2 - 10e_1 + e_4 - k_1 e_1 \\ \dot{e}_2 &= 28e_1 - e_2 - k_2 e_2 \\ \dot{e}_3 &= -\frac{8}{3}e_3 - k_3 e_3 \\ \dot{e}_4 &= -e_4 - k_4 e_4 \end{aligned} \tag{9}$$

To analyze the stability of the closed-loop error dynamics, the error equations obtained in Equation 9 are expressed in matrix form. This representation enables the stability of the system to be evaluated through eigenvalue analysis of the coefficient matrix.

In dynamical systems expressed in state-space form, system stability depends on the real parts of the eigenvalues of the coefficient matrix. Accordingly, if all eigenvalues have negative real parts, the error system is said to be asymptotically stable.

Accordingly, the error system is reformulated in state-space form as presented in Equation 10.

$$\begin{bmatrix} \dot{e}_1 \\ \dot{e}_2 \\ \dot{e}_3 \\ \dot{e}_4 \end{bmatrix} = \begin{bmatrix} -(10 + k_1) & 10 & 0 & 1 \\ 28 & -(1 + k_2) & 0 & 0 \\ 0 & 0 & -(8/3 + k_3) & 0 \\ 0 & 0 & 0 & -(k_4 + 1) \end{bmatrix} \begin{bmatrix} e_1 \\ e_2 \\ e_3 \\ e_4 \end{bmatrix} \tag{10}$$

Based on the coefficient matrix given in Equation 10, the eigenvalues of the system are obtained for the selected  $k$  values in order to examine the stability of the system. The characteristic equation, derived from the coefficient matrix in Equation 10 using the relation  $\det|(s * I - A)| = 0$  is presented in Equation 11.

$$((s + k_4 + 1)(3s + 3k_3 + 8)(11s + k_1 + 10k_2 + sk_1 + sk_2 + k_1k_2 + s^2 - 270))/3 = 0 \tag{11}$$

When the  $k_1 = k_2 = k_3 = k_4 = k$  values were taken to be equal, the resulting characteristic equation was subjected to the Routh–Hurwitz stability criterion, and it was determined that the system is stable for  $k > 11.82$ . For this purpose, in the initial stage, the control gains are selected as  $k_1 = k_2 = k_3 = k_4 = k = 2$ , and the eigenvalues of the system are examined. The obtained eigenvalues are  $\alpha_1 = -24,8$ ,  $\alpha_2 = 9,82$ ,  $\alpha_3 = -4,66$ , and  $\alpha_4 = -3$ . Since at least one eigenvalue has a positive real part, not all eigenvalues lie in the left half-plane. Therefore, the system is unstable for this selection of control gains. To stabilize the system, the control gains are then chosen as  $k_1 = k_2 = k_3 = k_4 = k = 18$ . For these gain values, the computed eigenvalues are  $\alpha_1 = -40.82$ ,  $\alpha_2 = -6.17$ ,  $\alpha_3 = -20.66$ , and  $\alpha_4 = -19$ . Since all eigenvalues possess negative real parts, the system matrix lies entirely in the left half-plane, indicating that the system is asymptotically stable under this parameter selection. This stability result demonstrates that synchronization of two identical Lorenz hyperchaotic systems can be successfully achieved using the proposed active control method.

### Numerical simulation results

In this section, the numerical simulation results related to the active synchronization of two identical Lorenz hyperchaotic systems are presented. First, the unstable case in which the selected control gains are insufficient

to achieve synchronization is examined. Subsequently, the stable case obtained with appropriately selected control gains is discussed. In this manner, the effect of the control gains on synchronization performance is comparatively evaluated.

### Numerical simulation results for the unstable case

In this stage, the control gains are selected as  $k_1 = k_2 = k_3 = k_4 = k = 2$ , and the synchronization behavior of the system is investigated. In the numerical simulations, the controller is initially deactivated and is activated at  $t = 10$  seconds. During the synchronization process, the initial conditions of the driver system are chosen as  $[2,2,2,2]$ , while those of the response system are selected as  $[8,8,8,8]$ . The time evolution of the state variables of the driver and response systems is presented in Figure 5.

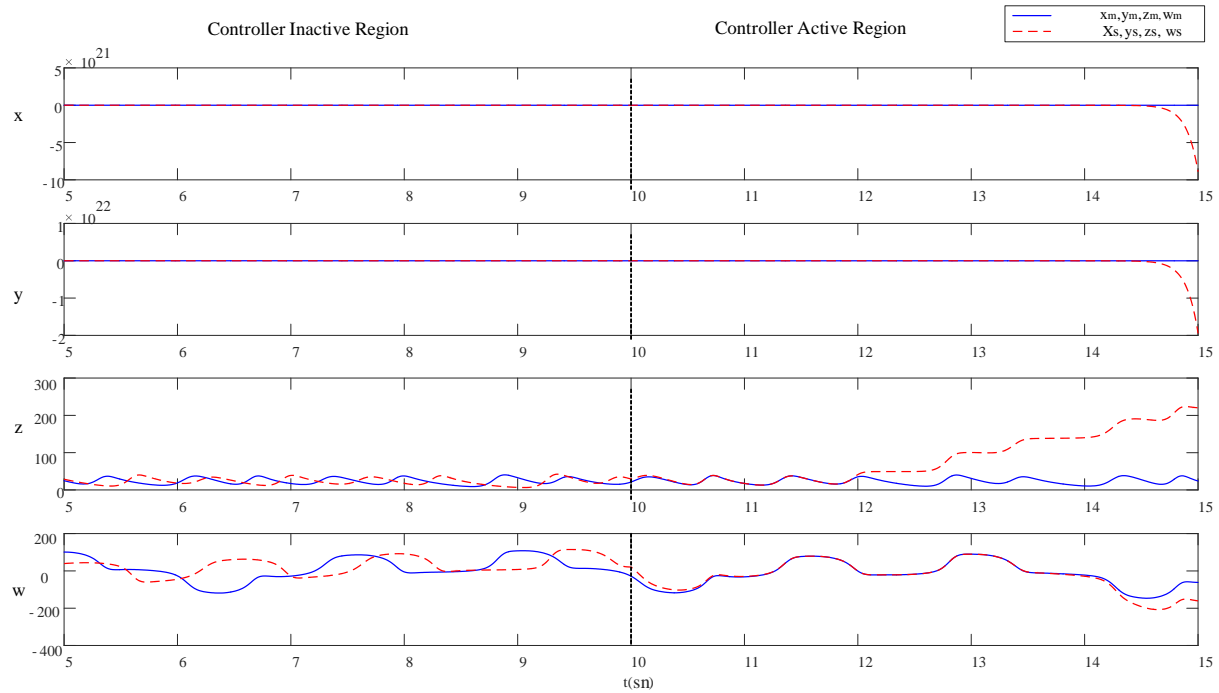


**Figure 5.** Time evolution of the state variables of the driver and response systems for the unstable case

During the initial time interval in which the controller is inactive, significant differences are observed between the state variables of the driver and response systems. Although the controller is activated after  $t = 10$  seconds, the selected gain values are insufficient, and therefore the system states do not converge to each other, resulting in failure of synchronization. In particular, growing oscillations are observed in some state variables, clearly indicating that synchronization is not achieved.

The time evolution of the error signals between the driver and response systems is presented in Figure 6.

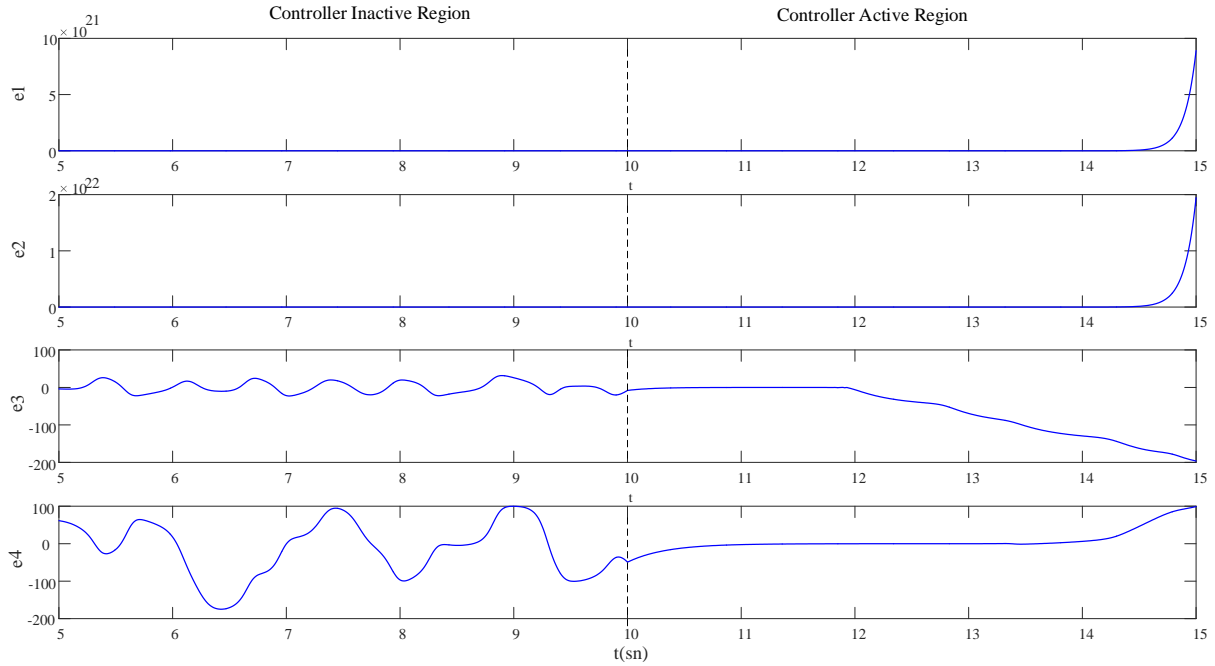


**Figure 6.** Time evolution of the error signals between the driver and response systems in the unstable case

The failure of the error signals to converge to zero clearly indicates that synchronization is not achieved. These results demonstrate that the selected gain values  $k_1 = k_2 = k_3 = k_4 = k = 2$  are insufficient to ensure system stability and successful synchronization.

### Numerical simulation results for the stable case

Following the unstable case analysis, the control gains are selected as  $k_1 = k_2 = k_3 = k_4 = k = 18$  in order to stabilize the system. In the numerical simulations, the controller is initially deactivated and is activated at  $t = 10$  seconds.

The initial conditions of the driver system are chosen as  $[2,2,2,2]$ , while the response system is initialized with  $[8,8,8,8]$ . The time evolution of the state variables of the driver and response systems is presented in Figure 7.

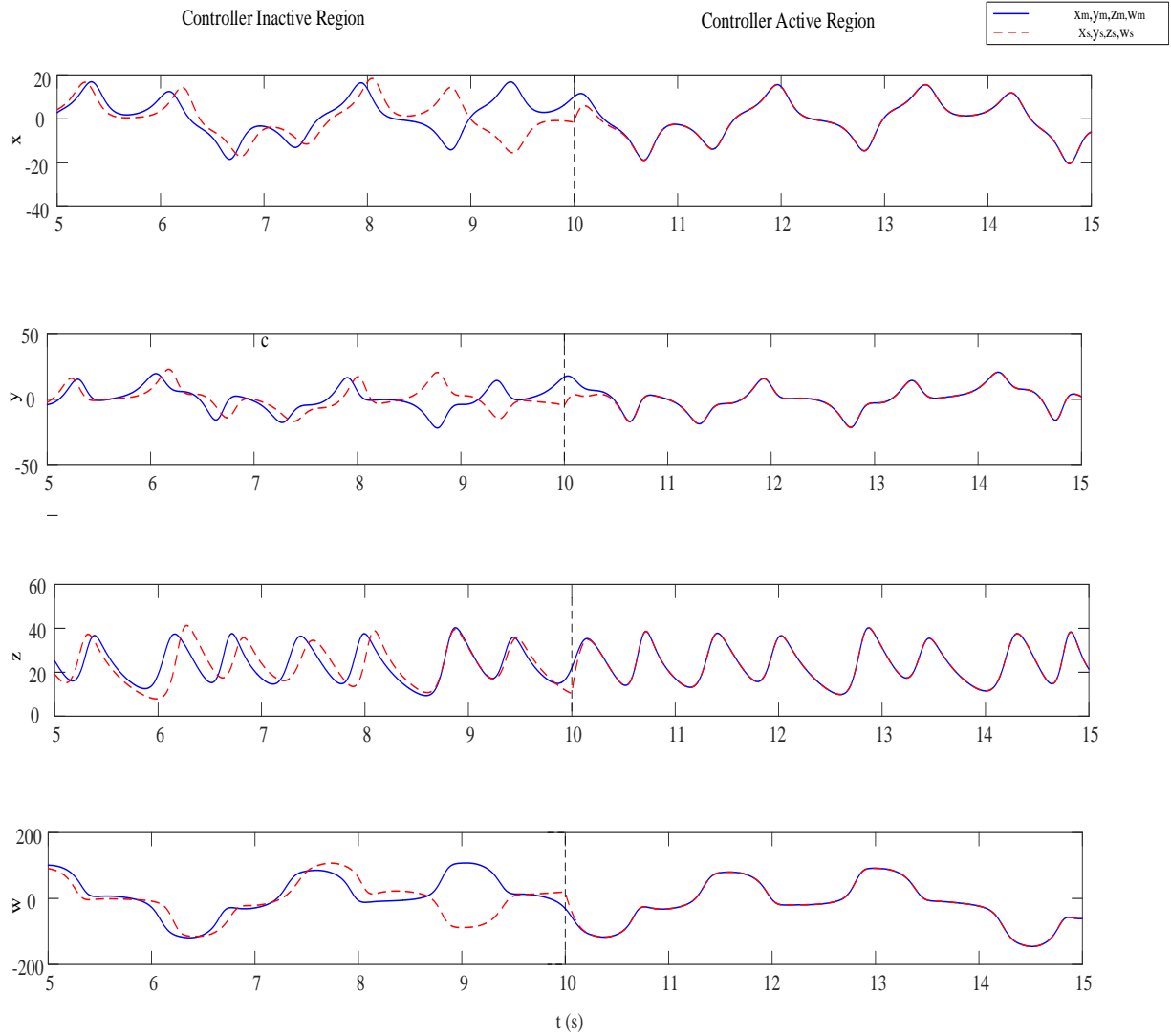


**Figure 7.** Time evolution of the state variables of the driver and response systems for the stable case

Before the controller is activated, significant discrepancies are observed between the two systems. After  $t = 10$  seconds, however, the effect of the control action causes the state variables to converge toward each other. As time progresses, the state variables of the driver and response systems overlap, clearly indicating that synchronization is successfully achieved.

The time evolution of the error signals between the driver and response systems is presented in Figure 8.

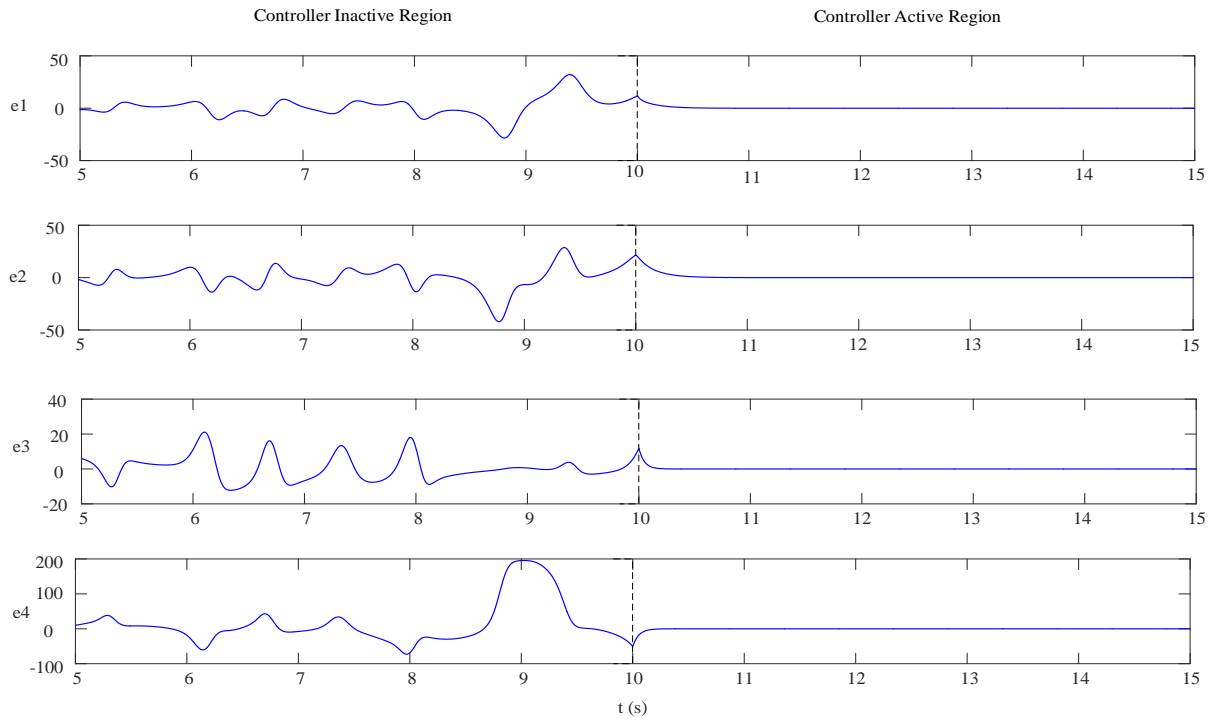


**Figure 8.** Time evolution of the error signals between the driver and response systems in the stable case

It is observed that the error signals converge to zero after the controller is activated, indicating that the system achieves asymptotic synchronization. These results demonstrate that the selected gain values  $k_1 = k_2 = k_3 = k_4 = k = 18$  are appropriate for ensuring system stability and successful synchronization.

#### 4. Signal Masking and Recovery Application

In this section, a hyperchaotic system-based signal masking and recovery application is implemented using the active synchronization approach. In order to evaluate the performance of the proposed structure under different input signals, the application is investigated through two distinct scenarios. In both cases, the information signal is masked by combining it with the chaotic signal generated from the driver hyperchaotic system and then transmitted through the communication channel. The synchronized response hyperchaotic system is employed at the receiver to recover and reconstruct the original information signal. In this framework, synchronization performance is very important for figuring out how accurate the masking and recovery processes are.

The block diagram of the proposed signal masking and recovery scheme is presented in Figure 9.

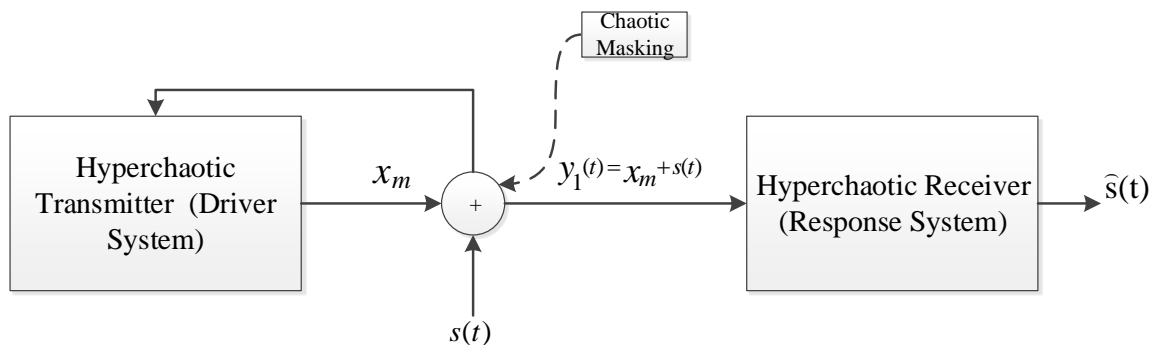


**Figure 9.** Block diagram of the active synchronization-based signal masking and recovery application

The input signal is defined as  $s(t) = 8 \cdot \sin(23t)$  in order to represent a signal suitable for modeling real-world analog data in terms of both frequency and amplitude components.

This signal is directly added to the state variable  $x_m(t)$  of the driver system, which serves as the reference during the synchronization process, to generate the masked (transmitted) signal. The applied masking operation is given in Equation 12.

$$y_1(t) = x_m(t) + s(t) \quad (12)$$

To recover the original information signal from the masked signal, the state variable  $x_s(t)$  of the response system is subtracted from the transmitted signal. In the proposed approach, the effectiveness of the masking and recovery mechanism directly depends on the accuracy of synchronization between the driver and response systems.

When synchronization is achieved, the equality  $x_m(t) = x_s(t)$  holds. Therefore, subtracting  $x_s(t)$  from the masked signal theoretically yields a recovered signal that coincides with the original input signal  $s(t)$ . The recovery operation is expressed in Equation 13.

$$\hat{s}(t) = y_1(t) - x_s(t) \quad (13)$$

The error signal  $e(t)$  is the difference between the input signal and the output signal that was recovered. The accuracy of synchronization is directly related to this error signal. As the synchronization between the driver and response systems gets better, the amplitude of the error signal gets smaller.

Theoretically, in the case of perfect synchronization, the error signal is expected to converge to zero. The mathematical expression corresponding to the defined error signal is given in Equation 14.

$$e(t) = s(t) - \hat{s}(t) \quad (14)$$

This application is implemented in the MATLAB environment. In the simulations, the initial conditions of the driver and response hyperchaotic systems are selected as [2,2,2,2] and [8,8,8,8], respectively. To demonstrate both the unsynchronized and synchronized states of the systems, the implementation is carried out in two stages. During the first time interval  $0 \leq t < 10$  s, no control action is applied, and the systems evolve freely in an unsynchronized manner. At  $t = 10$  s, the controller is activated with the control gains selected as  $k_1 = k_2 = k_3 = k_4 = k = 18$ . In this synchronized state, the applied gain value ensures that the synchronization error converges to zero, and complete synchronization between the systems is achieved. Under these conditions, the time evolutions of the input signal  $s(t)$ , the masked signal  $y_1(t)$ , the recovered signal  $\hat{s}(t)$ , and the error signal  $e(t)$  are presented in Figure 10.

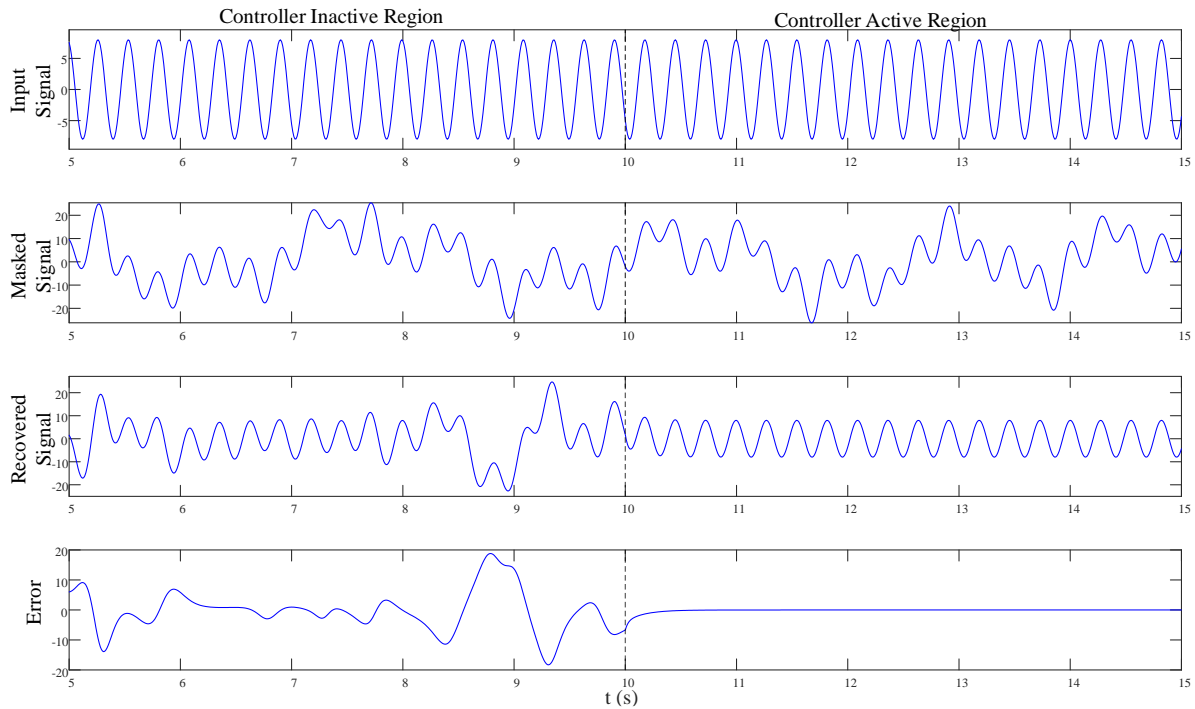


**Figure 10.** Time evolutions of the input, masked, recovered, and error signals in the first application scenario

As illustrated in Figure 10, the recovered signal fails to track the input signal correctly during the first 10 seconds when the controller isn't working. The error signal also shows clear oscillations with a large amplitude. This behaviour indicates that synchronization between the driver and response systems has not been achieved. Once the controller is activated at  $t = 10$  s, synchronization between the systems is established. Consequently, the recovered signal becomes consistent with the input signal. From this point onward, the error signal approaches zero in approximately 1 second, clearly demonstrating that the input signal is reconstructed with high accuracy. These results confirm that the proposed active synchronization-based approach operates effectively in signal masking and recovery applications.

To evaluate the performance of the proposed active synchronization-based masking and recovery scheme in more detail under different input signals, a second application scenario was implemented. In this case, a different information signal than the one used in the first application was selected to re-evaluate the system's masking and recovery performance. This allows analysing whether the proposed method is limited to a specific signal structure or whether it is also effective for input signals with different frequency and amplitude components.

In the second application, the input signal is selected as  $s(t) = 1.2 \cdot \sin(3t) + 5 \cdot \sin(2t)$ . Apart from this modification, the initial conditions of the driver and response hyperchaotic systems, the control gains, and the two-stage structure in which the controller is activated at  $t = 10$  s are kept identical to those used in the first application. In this way, the obtained results can be evaluated solely based on the change in the input signal. Under these conditions, the time evolutions of the input signal, masked signal, recovered signal, and error signal are presented in Figure 11.

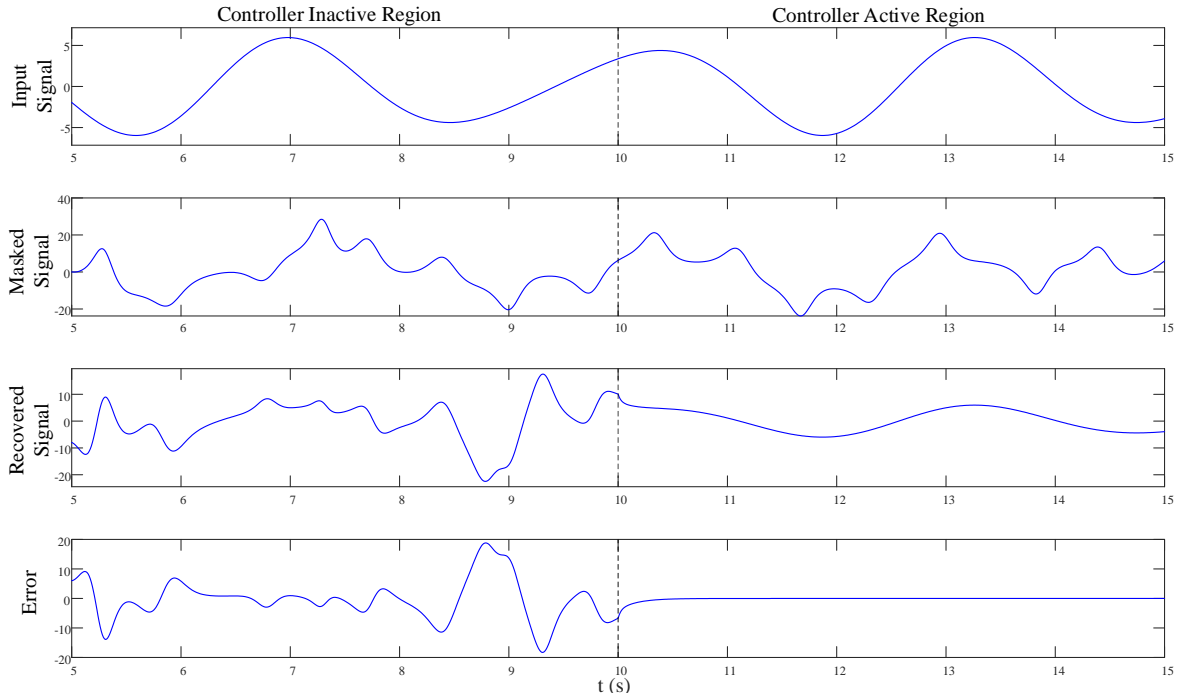


**Figure 11.** Time evolutions of the input, masked, recovered, and error signals in the second application scenario

As illustrated in Figure 11, it is observed that for a different information signal, the recovered signal exhibits a high degree of agreement with the input signal after the controller is activated, and the error signal approaches zero in approximately 1 second. This behavior shows that the driver and response hyperchaotic systems are in sync and that the information signal is accurately reconstructed from the masked signal. The results demonstrate that the proposed active synchronization-based method performs effectively and reliably for various information signals.

The outcomes from the two application scenarios in this section demonstrate that the active synchronization-based hyperchaotic system effectively masks and recovers signals. Both the driver and response systems are in sync after the controller is turned on. This enables accurate reconstruction of the information signal from the masked transmission. The fact that the error signal goes to zero shows that the suggested method is stable. Furthermore, the applicability of the proposed method to input signals with different frequency and amplitude components demonstrates its potential for use in various scenarios. However, it should be noted that implementing such systems in real-time applications will present certain challenges due to noise.

## 5. Conclusions

This study examined the Lorenz hyperchaotic system from a dynamical perspective, employing an active control strategy to achieve synchronization. Initial analysis of the system dynamics evaluated Lyapunov exponents, phase-space behavior, and sensitivity to initial conditions. The results unequivocally demonstrated that the system functions in a hyperchaotic domain, primarily as a result of the system's significant dependency on initial values and the existence of multiple positive Lyapunov exponents.

The synchronization challenge between two identical Lorenz hyperchaotic systems was formulated within the scope of active control once the dynamical behavior was established. It was demonstrated that choosing suitable control gains guarantees asymptotic stability of the entire system by building the error dynamics and conducting a stability evaluation. Eigenvalue evaluation also showed that all of the system matrix's eigenvalues are located in the left side of the complex plane with appropriate parameter adjustment, ensuring convergence and successful synchronization.

A signal masking and retrieval strategy based on the hyperchaotic system was created, building on the synchronized configuration. A comparative analysis of the system reactions before and after controller activation was conducted. The master (driving) and slave (response) systems were successfully synchronized when the control parameters were appropriately set. The embedded information signal was precisely recovered from the masked transmission under synchronized conditions, and the synchronization error gradually decreased to zero.

Two separate input signals with various amplitude and frequency characteristics were evaluated in order to further evaluate the resilience and flexibility of the suggested synchronization strategy. The active control-based synchronization framework is stable and reliable across different signal conditions, as shown by the consistent performance in both cases.

In general, the results show that active management can make the Lorenz hyperchaotic system work together. The synchronized structure is also a good base for apps that need to hide and get signals back. These findings illustrate the capability of hyperchaotic systems as efficient tools for information concealment and secure communication.

## **6. Author Contribution Statement**

Author 1 contributed to the preparation of the original draft, methodology development, simulation, and experimentation stages of the study. Author 2 conceptualized and supervised the study, and contributed to methodology refinement, writing, reviewing, and editing processes. Author 3 provided academic guidance, contributed to the theoretical framework, and participated in the reviewing and final editing of the manuscript.

## **7. Ethics Committee Approval and Conflict of Interest**

Ethics committee permission is not required for the prepared article. There is no conflict of interest with any person/institution in the prepared article.

## **8. Ethical Statement Regarding the Use of Artificial Intelligence**

During the writing process of this study, the artificial intelligence tool “ChatGPT,” developed by OpenAI, was used in a limited manner solely for linguistic editing purposes. The scientific content, analyses, and results are entirely the responsibility of the author(s).

## 9. References

- [1] S. H. Strogatz, *Nonlinear Dynamics and Chaos: With Applications to Physics, Biology, Chemistry, and Engineering*, 3rd ed. New York, NY, USA: Chapman and Hall/CRC, 2024.
- [2] G. Kolumban, M. P. Kennedy, and L. O. Chua, “The role of synchronization in digital communications using chaos. II. Chaotic modulation and chaotic synchronization,” *IEEE Trans. Circuits Syst. I, Fundam. Theory Appl.*, vol. 45, no. 11, pp. 1129–1140, Nov. 1998.
- [3] E. N. Lorenz, “Deterministic Nonperiodic Flow,” in *Universality in Chaos*, 2nd ed. New York, NY, USA: Routledge, 1989.
- [4] S. Banerjee and J. Kurths, “Chaos and Cryptography: A new dimension in secure communications,” *Eur. Phys. J. Spec. Top.*, vol. 223, no. 8, pp. 1441–1445, Jun. 2014.
- [5] L. Jin, J. Mei, and L. Li, “Chaos control of parametric driven Duffing oscillators,” *Appl. Phys. Lett.*, vol. 104, no. 13, p. 134101, Apr. 2014.
- [6] O. E. RöSSLer, “An equation for continuous chaos,” *Phys. Lett. A*, vol. 57, no. 5, pp. 397–398, Jul. 1976.
- [7] G. Chen, “Yet another chaotic attractor,” *Int. J. Bifurc. Chaos*, vol. 2, no. 3, pp. 705–708, 1993.
- [8] C. Liu, T. Liu, L. Liu, and K. Liu, “A new chaotic attractor,” *Chaos Solitons Fractals*, vol. 22, no. 5, pp. 1031–1038, Dec. 2004.
- [9] A. Xiong, X. Zhao, J. Han, and G. Liu, “Application of the Chaos Theory in the Analysis of EMG on Patients with Facial Paralysis,” in *Robot Intelligence Technology and Applications 2: Results from the 2nd International Conference on Robot Intelligence Technology and Applications*, J.-H. Kim, E. T. Matson, H. Myung, P. Xu, and F. Karray, Eds. Cham, Switzerland: Springer, 2014, pp. 805–819.
- [10] Z. Huang, W. Dong, H. Duan, and H. Li, “Similarity Measure Between Patient Traces for Clinical Pathway Analysis: Problem, Method, and Applications,” *IEEE J. Biomed. Health Inform.*, vol. 18, no. 1, pp. 4–14, Jan. 2014.
- [11] Z. Kang, J. Sun, L. Ma, Y. Qi, and S. Jian, “Multimode Synchronization of Chaotic Semiconductor Ring Laser and its Potential in Chaos Communication,” *IEEE J. Quantum Electron.*, vol. 50, no. 3, pp. 148–157, Mar. 2014.
- [12] M. L. Barakat, A. S. Mansingka, A. G. Radwan, and K. N. Salama, “Hardware stream cipher with controllable chaos generator for colour image encryption,” *IET Image Process.*, vol. 8, no. 1, pp. 33–43, 2014.
- [13] A. Anees, A. M. Siddiqui, and F. Ahmed, “Chaotic substitution for highly autocorrelated data in encryption algorithm,” *Commun. Nonlinear Sci. Numer. Simul.*, vol. 19, no. 9, pp. 3106–3118, Sep. 2014.
- [14] Y. Ji *et al.*, “Microwave-Photonic Sensor for Remote Water-Level Monitoring Based on Chaotic Laser,” *Int. J. Bifurc. Chaos*, vol. 24, no. 3, p. 1450032, Mar. 2014.
- [15] M. Awais, M. A. Khan, and Z. Bashir, “Exploring the stochastic patterns of hyperchaotic Lorenz systems with variable fractional order and radial basis function networks,” *Clust. Comput.*, vol. 27, no. 7, pp. 9031–9064, Oct. 2024.
- [16] O. E. Rossler, “An equation for hyperchaos,” *Phys. Lett. A*, vol. 71, no. 2, pp. 155–157, Apr. 1979.
- [17] L. M. Pecora and T. L. Carroll, “Synchronization in chaotic systems,” *Phys. Rev. Lett.*, vol. 64, no. 8, pp. 821–824, Feb. 1990.
- [18] A. Khan and M. Shahzad, “Synchronization of circular restricted three body problem with Lorenz hyper chaotic system using a robust adaptive sliding mode controller,” *Complexity*, vol. 18, no. 6, pp. 58–64, 2013.
- [19] H.-K. Chen, “Global chaos synchronization of new chaotic systems via nonlinear control,” *Chaos Solitons Fractals*, vol. 23, no. 4, pp. 1245–1251, Feb. 2005.
- [20] H.-H. Chen, “Global synchronization of chaotic systems via linear balanced feedback control,” *Appl. Math. Comput.*, vol. 186, no. 1, pp. 923–931, Mar. 2007.
- [21] P. He, C.-G. Jing, T. Fan, and C.-Z. Chen, “Robust decentralized adaptive synchronization of general complex networks with coupling delayed and uncertainties,” *Complexity*, vol. 19, no. 3, pp. 10–26, 2014.

- [22] R. Rakkiyappan and N. Sakthivel, “Cluster synchronization for T–S fuzzy complex networks using pinning control with probabilistic time-varying delays,” *Complexity*, vol. 21, no. 1, pp. 59–77, 2015.
- [23] I. Ahmad, A. B. Saaban, A. B. Ibrahim, and M. Shahzad, “Global Chaos Identical and Nonidentical Synchronization of a New 3-D Chaotic Systems Using Linear Active Control,” *Asian J. Appl. Sci.*, vol. 2, no. 1.
- [24] M. T. Akter, A. Tammim, and S. Hussien, “Chaos control and synchronization of modified Lorenz system using active control and backstepping scheme,” *Waves Random Complex Media*, pp. 1–20, May 2023.
- [25] A. Durdu and Y. Uyaroglu, “Comparison of synchronization of chaotic Burke-Shaw attractor with active control and integer-order and fractional-order P-C method,” *Chaos Solitons Fractals*, vol. 164, p. 112646, Nov. 2022.
- [26] A. Tammim and M. T. Akter, “Shimizu–Morioka’s chaos synchronization: An efficacy analysis of active control and backstepping methods,” *Front. Appl. Math. Stat.*, vol. 9, Apr. 2023.
- [27] Y. Zhou, Y. Guo, W. Zhang, and P. Zhao, “Novel Hyperchaotic System with Linear Memristor: Active Synchronization and an Image Encryption Application,” *Nonlinear Dyn.*, vol. 113, no. 22, pp. 31669–31689, Nov. 2025.
- [28] M. Kopp and I. Samuilik, “A New 6D Two-wing Hyperchaotic System: Dynamical Analysis, Circuit Design, and Synchronization,” *Chaos Theory Appl.*, vol. 6, no. 4, pp. 273–283, Nov. 2024.
- [29] E. Ozpolat, V. Celik, and A. Gulten, “A Novel Four-Dimensional Hyperchaotic System: Design, Dynamic Analysis, Synchronization, and Image Encryption,” *IEEE Access*, vol. 12, pp. 126063–126073, 2024.
- [30] A. S. Lekshmi, V. Balakumar, and D. Cafagna, “On the dynamics and synchronization of a new fractional-order hyperchaotic system,” *Int. J. Dyn. Control*, vol. 14, no. 1, p. 16, Dec. 2025.
- [31] X. Wang and M. Wang, “A hyperchaos generated from Lorenz system,” *Physica A*, vol. 387, no. 14, pp. 3751–3758, 2008.
- [32] H. D. I. Abarbanel, R. Brown, and M. B. Kennel, “Lyapunov Exponents in Chaotic Systems: Their Importance and Their Evaluation Using Observed Data,” *Int. J. Mod. Phys. B*, vol. 5, pp. 1347–1375, Jan. 1991.
- [33] A. Wolf, J. B. Swift, H. L. Swinney, and J. A. Vastano, “Determining Lyapunov exponents from a time series,” *Physica D*, vol. 16, no. 3, pp. 285–317, Jul. 1985.
- [34] M. Baia, F. Bagnoli, T. Matteuzzi, and A. Pikovsky, “Synchronization of branching chain of dynamical systems,” *Physica D*, vol. 477, p. 134664, Jul. 2025.
- [35] F. Setoudeh, M. M. Dezhidar, and M. Najafi, “Nonlinear analysis and chaos synchronization of a memristive-based chaotic system using adaptive control technique in noisy environments,” *Chaos Solitons Fractals*, vol. 164, p. 112710, 2022.
- [36] H. Cheng, H. Li, Q. Dai, and J. Yang, “A deep reinforcement learning method to control chaos synchronization between two identical chaotic systems,” *Chaos Solitons Fractals*, vol. 174, p. 113809, 2023.
- [37] L. O. Chua, M. Itoh, L. Kocarev, and K. Eckert, “Chaos Synchronization in Chua’s Circuit,” *J. Circuits Syst. Comput.*, vol. 3, no. 1, pp. 93–108, Mar. 1993.
- [38] M. T. Yassen, “Chaos synchronization between two different chaotic systems using active control,” *Chaos Solitons Fractals*, vol. 23, no. 1, pp. 131–140, Jan. 2005.